Artificial Layer Enable In-situ generation of Homogeneous Inorganic/Organic Composites Solid Electrolyte Interphase for Stable Lithium Metal Batteries

Huajun Tian[a], Jianxun Zhang[a], Bijiao He[a], Yang Liu[a], Weiyi Li[a], Fang Zhang[a], Zile Wang[a], Xuewei Lu[a], Yan Xin[a], Shuwei Wang[a]*

[a]Key Laboratory of Power Station Energy Transfer Conversion and System of Ministry of Education and School of Energy Power and Mechanical Engineering, and Beijing Laboratory of New Energy Storage Technology, North China Electric Power University, Beijing, 102206, China

Corresponding Authors:
E-mail: 50202718@ncepu.edu.cn

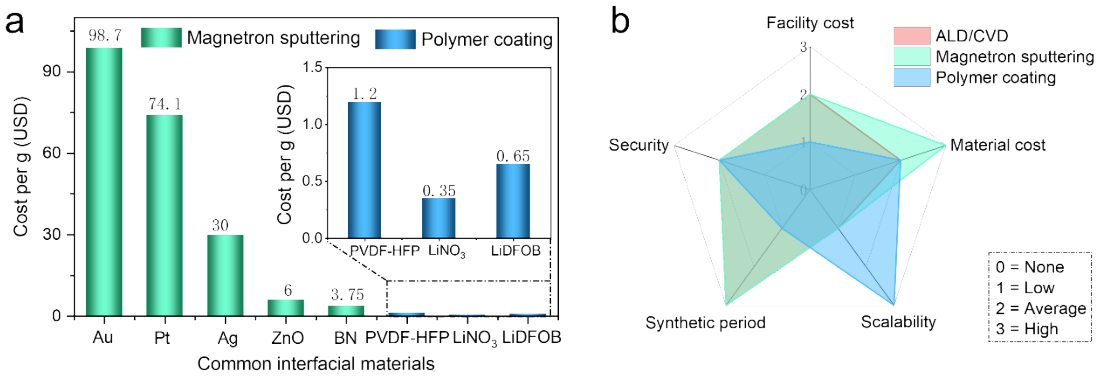

Figure S1. (a) Estimated unit prices of different raw materials of common interfacial materials used in magnetron sputtering and polymer coating process. (b) Main properties of commonly adopted methods to construct artificial SEI.

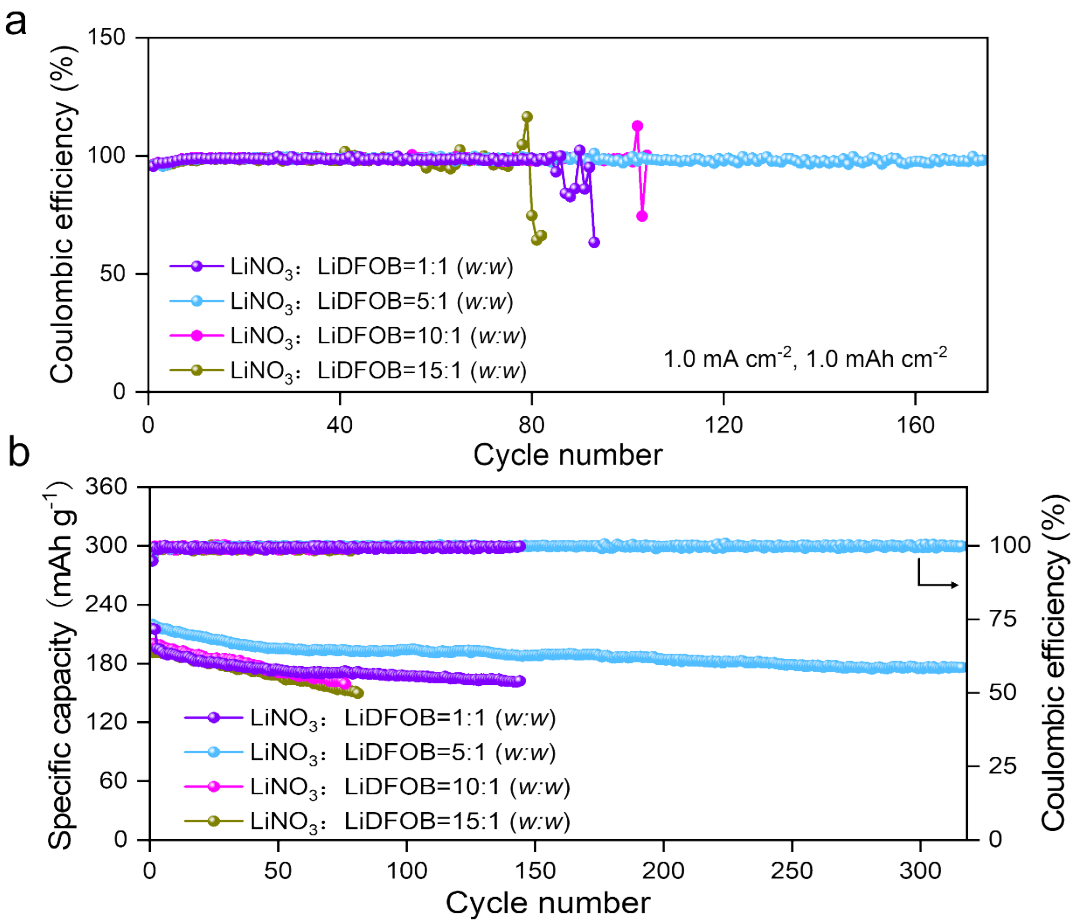

Figure S2. Comparison of electrochemical performances of half cell and full cell with different ratio of Li salts.

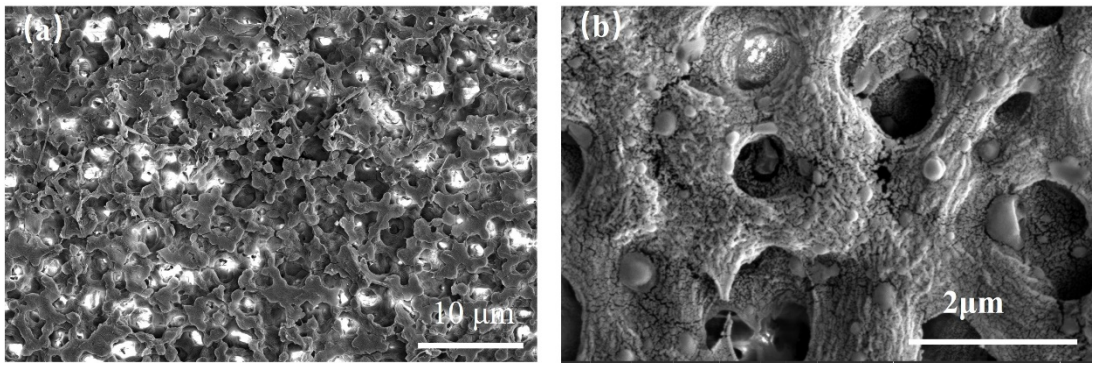

Figure S3. SEM images of PNL layer with different magnifications.

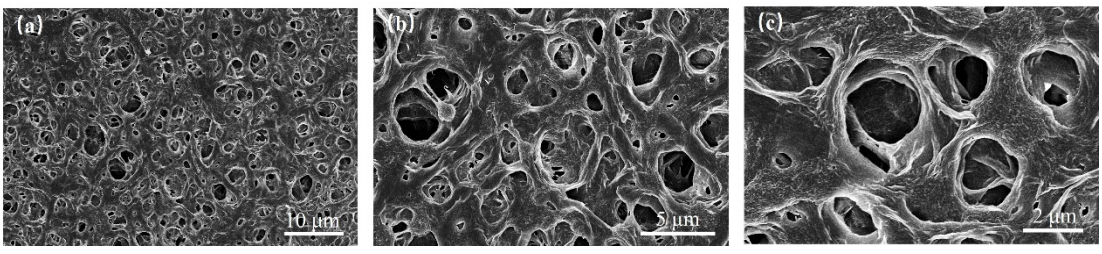

Figure S4. SEM images of pure layer with different magnifications.

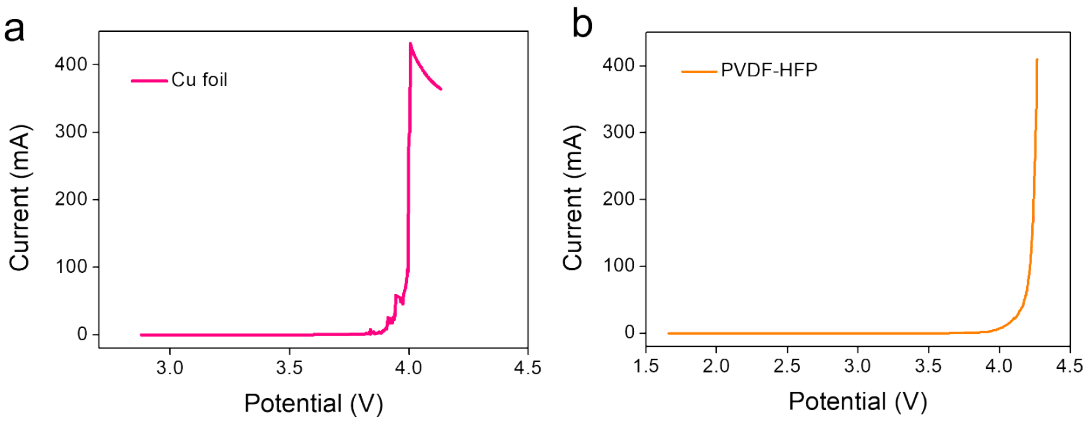

Figure S5. Positive linear sweep voltammograms (LSV) sweep to test the oxidation stabilities of bare Cu foil without protection (a) and pure layer (b) in Li||stainless-steel cells at a scanning rate of 0.1 mV s^{-1}.

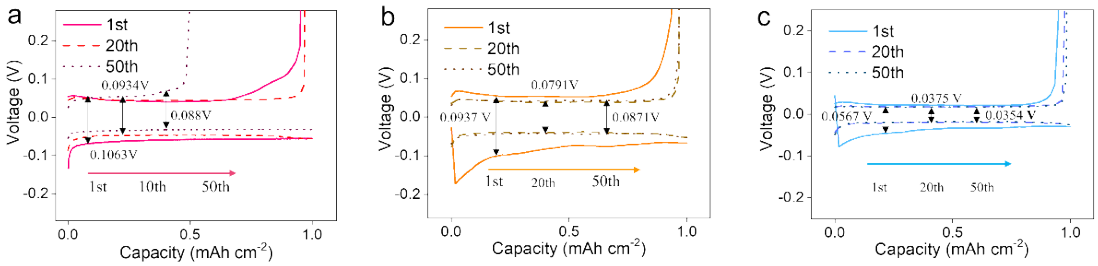

Figure S6. Voltage capacity profiles of different cycles of (a) bare Cu foil, (b) pure and (c) PNF layers modified at 1.0 mA cm^{-2} for 1.0 mAh cm^{-2}.

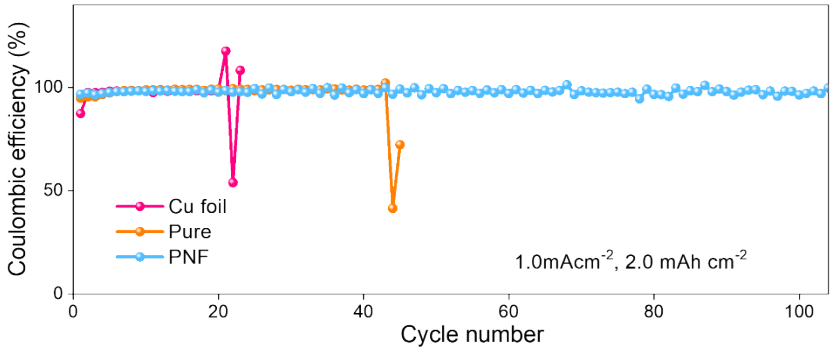

Figure S7. Coulombic efficiency of repeated Li plating/stripping at 1.0 mA cm^{-2} for 2 h on bare Cu foil and Cu foil covered by pure and PNF layer.

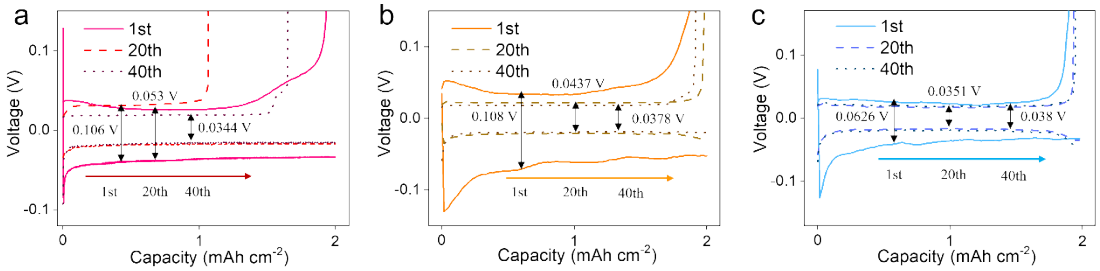

Figure S8. Voltage capacity profiles of different cycles of (a) bare Cu foil, (b) pure and (c) PNF layers modified at 1.0 mA cm^{-2} for 2.0 mAh cm^{-2}.

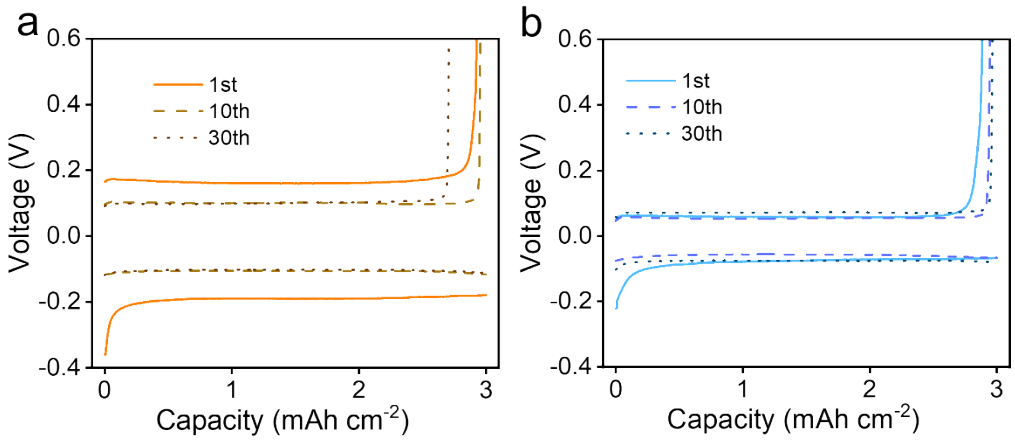

Figure S9. Voltage capacity profiles of different cycles of (a) pure and (b) PNF layers modified at 3.0 mA cm^{-2} for 3.0 mAh cm^{-2}.

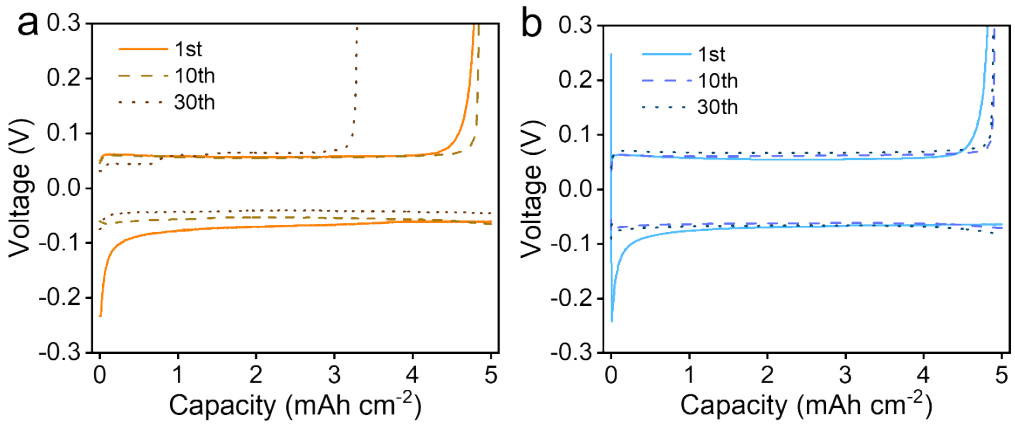

Figure S10. Voltage capacity profiles of different cycles of (a) pure and (b) PNF layers modified at 5.0 mA cm^{-2} for 5.0 mAh cm^{-2}.

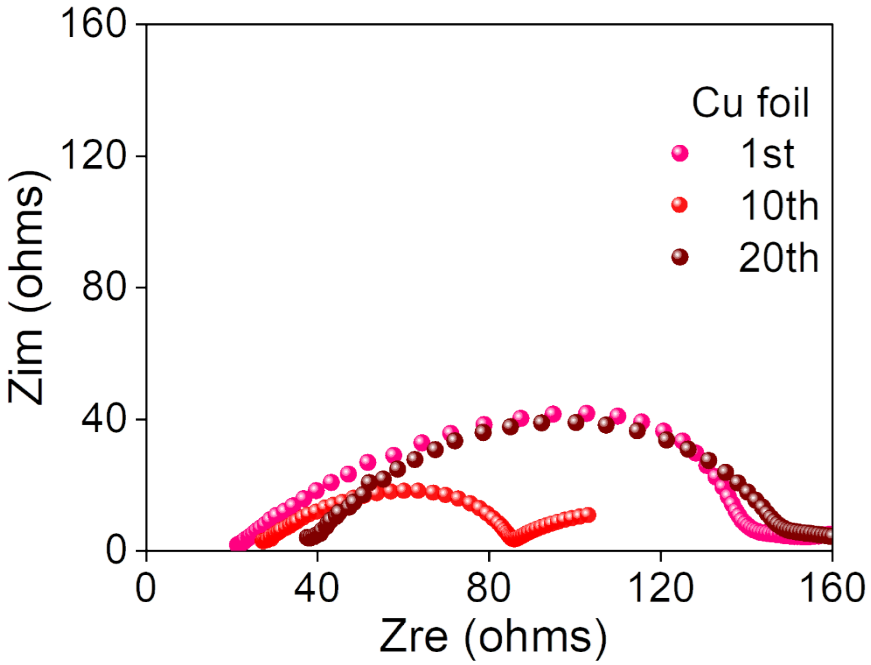

Figure S11. Nyquist plots of three styles of anodes after different cycles of bare Li‖Cu cells.

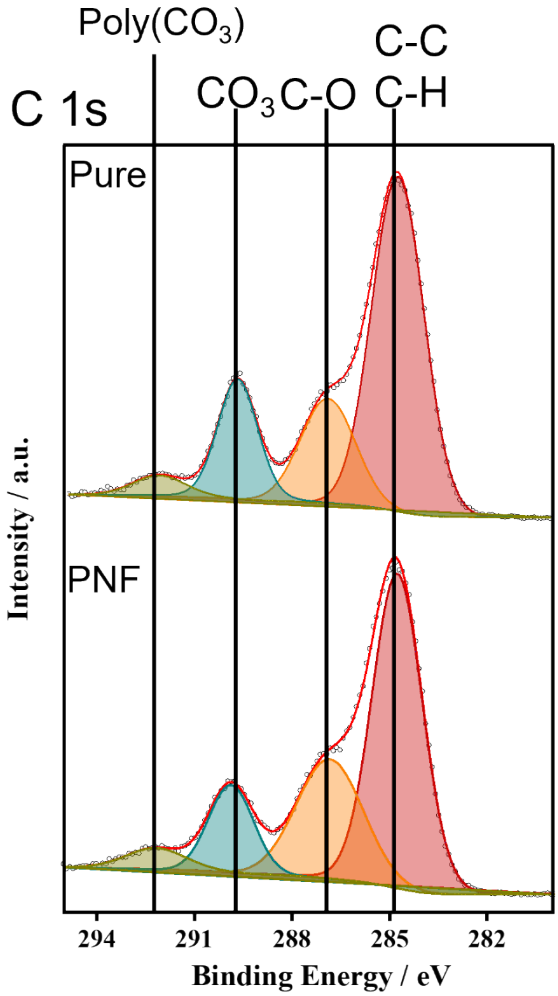

Figure S12. XPS C 1s spectrum of the SEIs after Li plating with pure and PNF layers modified.

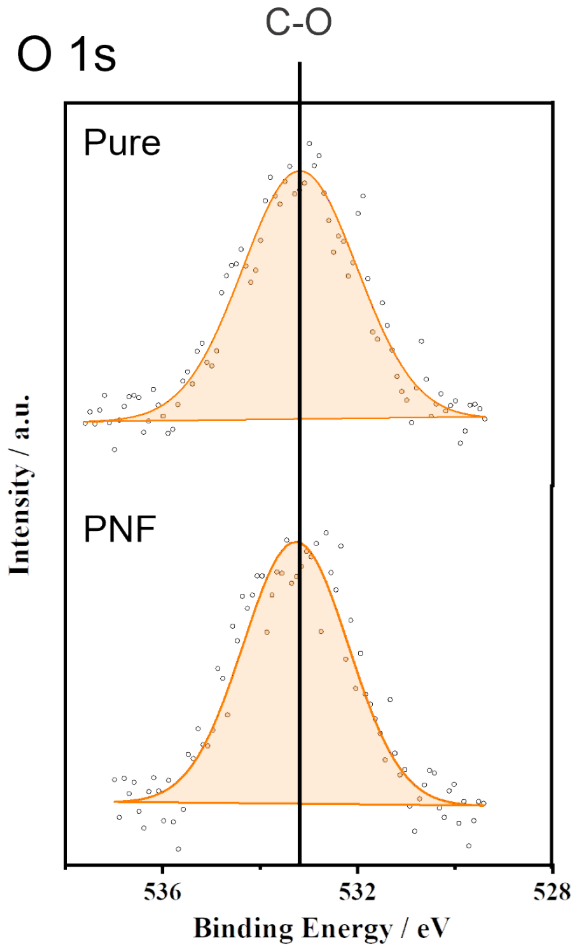

Figure S13. XPS O 1s spectrum of the SEIs after Li plating with pure and PNF layers modified.

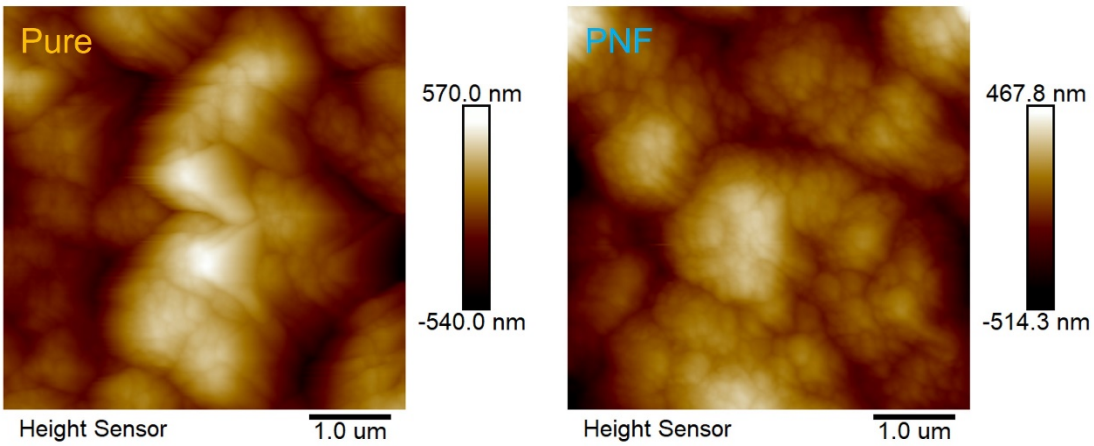

Figure S14. AFM images of SEI on Li metal after plating at 1.0 mA cm^{-2} for 1 h (1.0 mAh cm^{-2}) with pure and PNF layers modified.

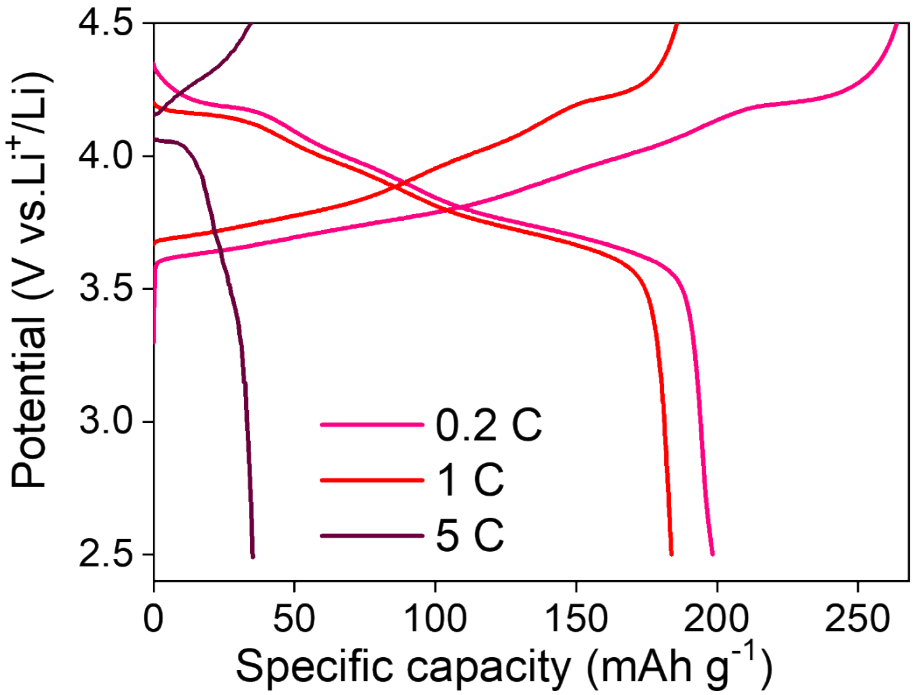

Figure S15. Charge/discharge profiles of the full cells at different rates.

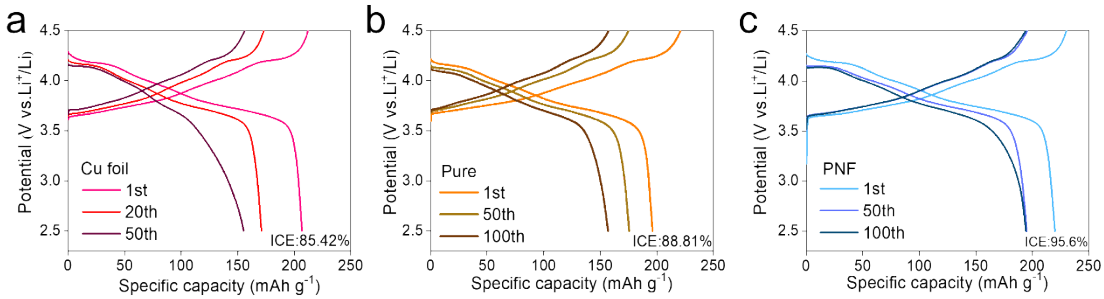

Figure S16. Charge/discharge profiles of the full cells at different cycles.

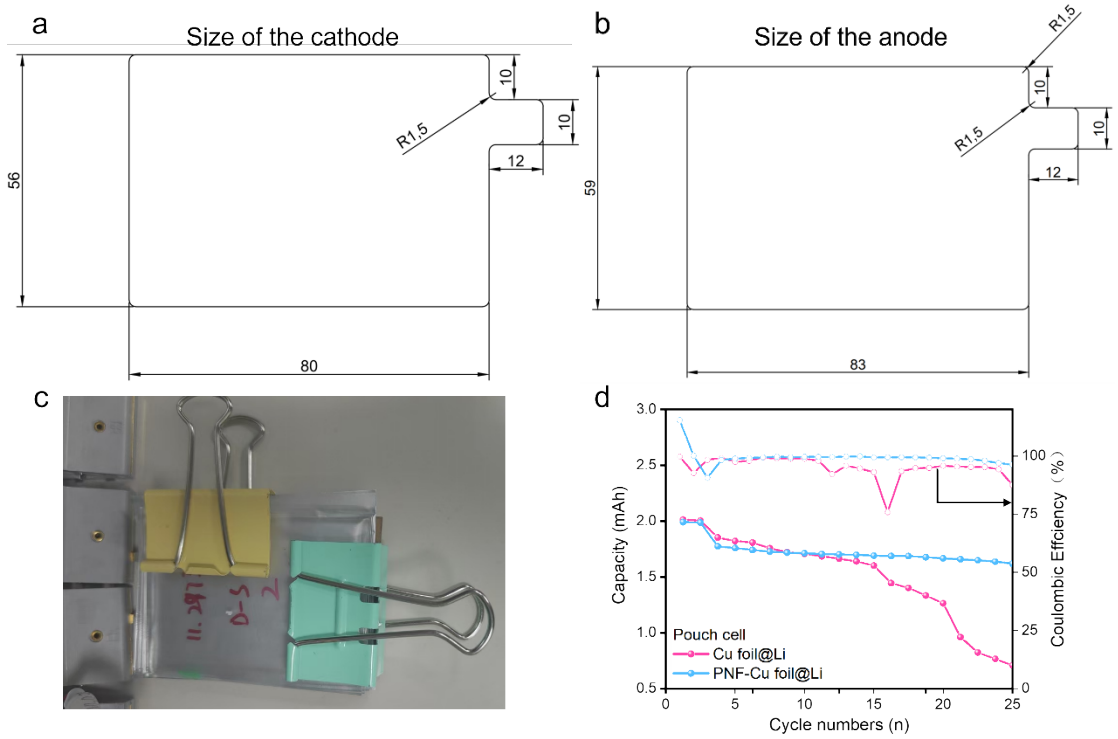

Figure S17. (a-b) The sized of the electrodes in pouch cells. (c) The optical image of pouch cell assembled in laboratory. (d) Electrochemical performance of PNF layer based pouch cell.

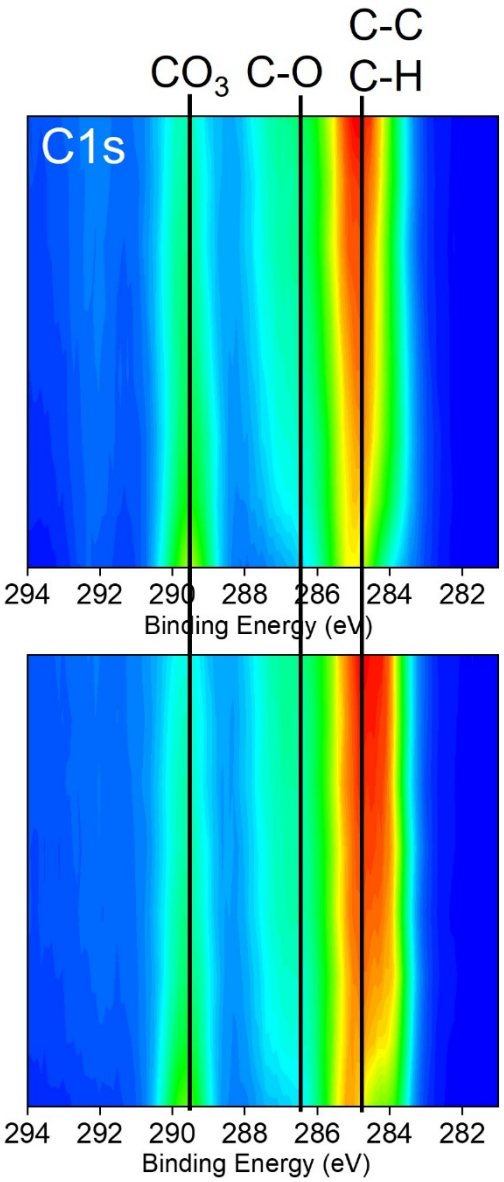

Figure S18. XPS C 1s depth profiles of the CEI layers on NCM811 electrodes after 10 cycles.

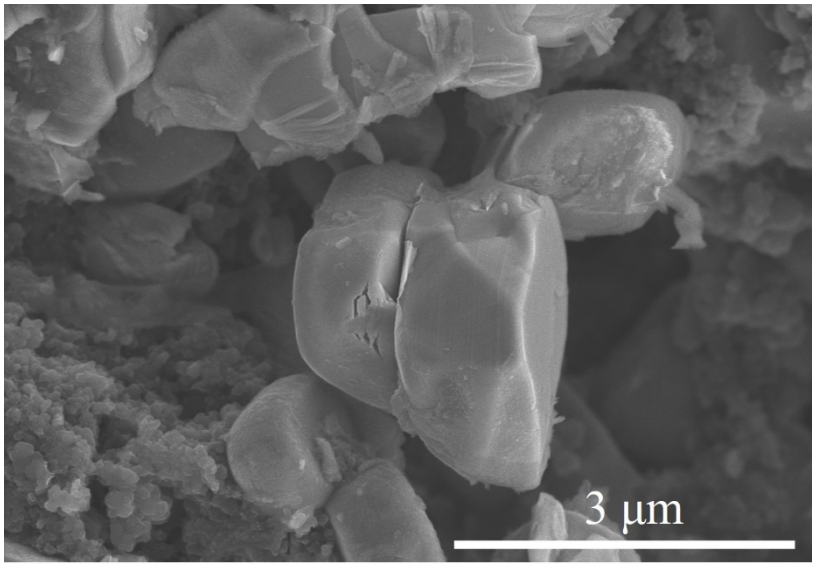

Figure S19. SEM image of cycled NCM811 cathodes in pure layer modified system.

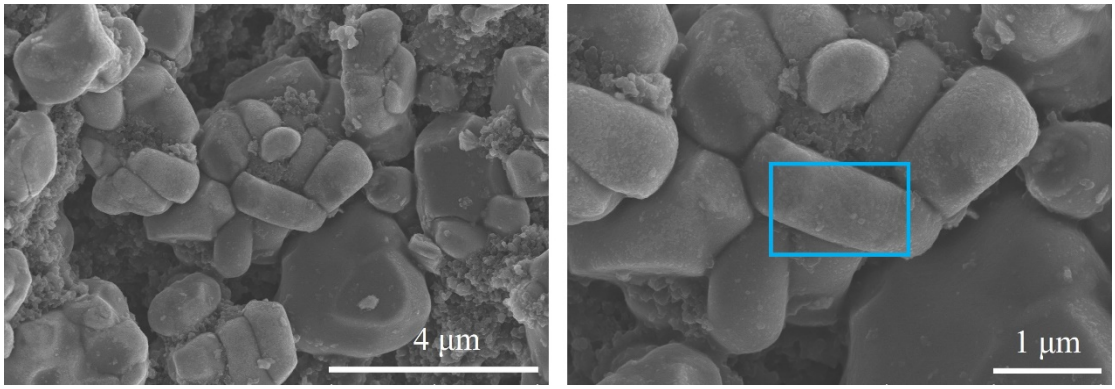

Figure S20. SEM image of cycled NCM811 cathodes in PNL layer modified system.

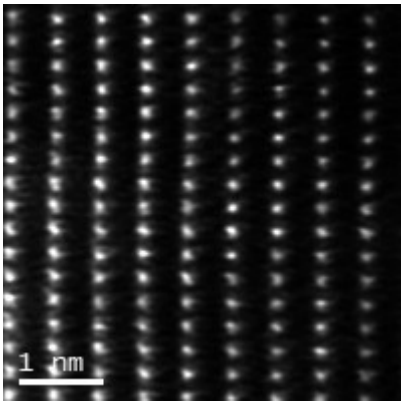

Figure S21. The typical structure of layered phase.

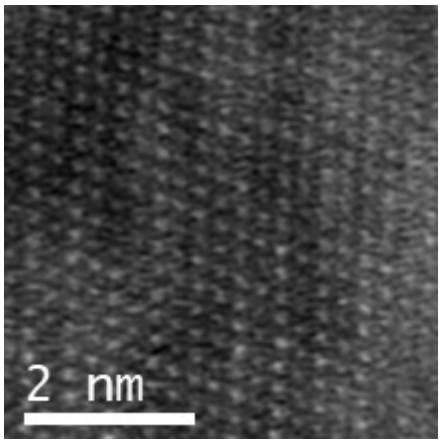

Figure S22. The typical structure of rock-salt phase.

Table R1. Electrochemical performances of CNF/nc-TNO@Li||NCM811 full cells and those of recently reported high-voltage Li metal batteries (LMBs).

Artificial SEI	Cathode	High voltage	Initial capacity	Capacity retention	Ref.
PNF	$LiNi_{0.8}Co_{0.1}Mn_{0.1}O_2$	4.5 V	218.6 mAh g^{-1} (0.5 C)	80.3 % (300^{th}) 84.3% (200^{th}) 88.7% (100^{th})	This work
LiCN/LiF/ polyamino nitriles	$LiNi_{0.8}Co_{0.15}Al_{0.05}O_2$	4.2 V	190.2 mAh g^{-1} (0.2 C)	88.2 % (100^{th})	[1]
YF_3/PMMA	$LiNi_{0.8}Co_{0.1}Mn_{0.1}O_2$	4.3 V	194.0 mAh g^{-1} (1 C)	83.78 % (200^{th})	[2]
$Ti_3C_2T_x$ MXene	$LiNi_{0.5}Co_{0.2}Mn_{0.3}O_2$	4.25 V	165 mAh g^{-1} (0.2C)	83 % (200^{th})	[3]
PDOL/(rGO)	$LiNi_{0.6}Co_{0.2}Mn_{0.2}O_2$	4.3V	173.5 mAh g^{-1} (0.3C)	86 % (100^{th})	[4]
$LiAlO_2$	$LiNi_{0.8}Co_{0.1}Mn_{0.1}O_2$	4.2 V	185 mAh g^{-1} (1 C)	82.4 % (200^{th})	[5]
Mo_6S_8/carbon	$LiNi_{0.8}Co_{0.1}Mn_{0.1}O_2$	4.3 V	160 mAh g^{-1} (1 C)	63 % (200^{th})	[6]
PVA polymer	$LiNi_{0.6}Co_{0.2}Mn_{0.2}O_2$	4.2V	175 mAh g^{-1} (0.5 C)	74.5 % (120^{th})	[7]
sodium alginate	$LiNi_{0.6}Co_{0.2}Mn_{0.2}O_2$	4.3 V	120.5 mAh g^{-1} (0.5 C)	93.8 % (200^{th})	[8]
$LiZrO(NO_3)_2$	$LiCoO_2$	4.3 V	138.8 mAh g^{-1} (0.5 C)	72.4 % (100^{th})	[9]
$CsPF_6$	$LiNi_{0.6}Co_{0.2}Mn_{0.2}O_2$	4.3 V	155 mAh g^{-1} (0.1 C)	75 % (120^{th})	[10]
PEGDA/LiDFOB	$LiNi_{0.8}Co_{0.1}Mn_{0.1}O_2$	4.3 V	206.7 mAh g^{-1} (0.5 C)	58.4 % (300^{th})	[11]
$AgSCF_3$	$LiCoO_2$	4.6V	205.5 mAh g^{-1} (0.1C)	63.3 % (200^{th})	[12]

References

[1] X. Chen, M. Shang, J. Niu, Pre-Solid Electrolyte Interphase-Covered Li Metal Anode with Improved Electro-Chemo-Mechanical Reliability in High-Energy-Density Batteries, ACS Applied Materials & Interfaces 13 (2021) 34064-34073. https://doi.org/10.1021/acsami.1c05966.

[2] Y. Zhang, R. Qiao, Q. Nie, P. Zhao, Y. Li, Y. Hong, S. Chen, C. Li, B. Sun, H. Fan, J. Deng, J. Xie, F. Liu, J. Song, Synergetic regulation of SEI mechanics and crystallographic orientation for stable lithium metal pouch cells, Nature Communications 15 (2024) 4454. https://doi.org/10.1038/s41467-024-48889-8.

[3] X. Chen, M. Shang, J. Niu, Inter-layer-calated Thin Li Metal Electrode with Improved Battery Capacity Retention and Dendrite Suppression, Nano Letters 20 (2020) 2639-2646. https://doi.org/10.1021/acs.nanolett.0c00201.

[4] R. Li, J. Li, L.-x. Li, H. Yang, G. Zhang, J. Xiang, X.-q. Shen, M.-x. Jing, A bifunctional composite artificial solid electrolyte interphase for high stable solid-state lithium batteries, Colloids and Surfaces A: Physicochemical and Engineering Aspects 657 (2023) 130600. https://doi.org/https://doi.org/10.1016/j.colsurfa.2022.130600.

[5] X. Hu, Y. Ma, J. Qian, W. Qu, Y. Li, R. Luo, H. Wang, A. Zhou, Y. Chen, K. Shi, L. Li, F. Wu, R. Chen, Self-Induced Dual-Layered Solid Electrolyte Interphase with High Toughness and High Ionic Conductivity for Ultra-Stable Lithium Metal Batteries, Advanced Materials 36 (2024) 2303710. https://doi.org/https://doi.org/10.1002/adma.202303710.

[6] K. Lu, S. Gao, R.J. Dick, Z. Sattar, Y. Cheng, A fast and stable Li metal anode incorporating an Mo₆S₈ artificial interphase with super Li-ion conductivity, JOURNAL OF MATERIALS CHEMISTRY A 7 (2019) 6038-6044. https://doi.org/10.1039/c8ta12450g.

[7] Y. Zhao, D. Wang, Y. Gao, T. Chen, Q. Huang, D. Wang, Stable Li metal anode by a polyvinyl alcohol protection layer via modifying solid-electrolyte interphase layer, Nano Energy 64 (2019) 103893. https://doi.org/https://doi.org/10.1016/j.nanoen.2019.103893.

[8] J. Jeong, J. Lee, J. Kim, J. Chun, D. Kang, S.M. Han, C. Jo, J. Lee, A biopolymer-based functional separator for stable Li metal batteries with an additive-free commercial electrolyte, JOURNAL OF MATERIALS CHEMISTRY A 9 (2021) 7774-7781. https://doi.org/10.1039/d0ta12153c.

[9] C. Chen, Q. Liang, G. Wang, D. Liu, X. Xiong, Grain-Boundary-Rich Artificial SEI Layer for High-Rate Lithium Metal Anodes, Advanced Functional Materials 32 (2022) 2107249. https://doi.org/https://doi.org/10.1002/adfm.202107249.

[10] S. Tang, Q. Mei, Y. Zhai, Y. Liu, Cation-polymerized artificial SEI layer modified Li metal applied in soft-matter polymer electrolyte, Nanotechnology 35 (2024) 335401. https://doi.org/10.1088/1361-6528/ad49ad.

[11] W. Cao, J. Lu, K. Zhou, G. Sun, J. Zheng, Z. Geng, H. Li, Organic-inorganic composite SEI for a stable Li metal anode by in-situ polymerization, Nano Energy 95 (2022) 106983. https://doi.org/https://doi.org/10.1016/j.nanoen.2022.106983.

[12] C. Xu, S. Zhang, C. Chen, Y. Lin, B. Qu, H. Zhou, M. Wu, Rational construction Ag/LiF/sulfide rich protective layer for remarkably enhancing the stability of Li metal anodes, Chemical Engineering Journal 482 (2024) 148914. https://doi.org/https://doi.org/10.1016/j.cej.2024.148914.